DLC-1, a Rho GTPase-activating protein with tumor suppressor function, is essential for embryonic development

Marian E. Durkin[a,*], Miriam R. Avner[b], Chang-Goo Huh[a], Bao-Zhu Yuan[a,1], Snorri S. Thorgeirsson[a], Nicholas C. Popescu[a,*]

[a] *Laboratory of Experimental Carcinogenesis, National Cancer Institute, National Institutes of Health, 37 Convent Drive, Bethesda, MD 20892, USA*
[b] *Pathology/Histotechnology Laboratory, Veterinary Pathology Section, SAIC-Frederick, National Cancer Institute at Frederick, Frederick, MD 21702, USA*

Received 12 November 2004; revised 21 December 2004; accepted 29 December 2004

Available online 19 January 2005

Edited by Michael R. Bubb

Abstract DLC-1 (deleted in liver cancer 1) is a Rho GTPase-activating protein that is able to inhibit cell growth and suppress tumorigenesis. We have used homologous recombination to inactivate the mouse DLC-1 gene (*Arhgap7*). Mice heterozygous for the targeted allele were phenotypically normal, but homozygous mutant embryos did not survive beyond 10.5 days post coitum. Histological analysis revealed that DLC-1$^{-/-}$ embryos had defects in the neural tube, brain, heart, and placenta. Cultured fibroblasts from DLC-1-deficient embryos displayed alterations in the organization of actin filaments and focal adhesions.

Keywords: Rho GTPase-activating protein; Knock-out mouse; Embryonic lethal

1. Introduction

The Rho GTPase-activating proteins (GAPs) are negative regulators of the Rho family of small GTPases, which control cellular processes such as proliferation, cytoskeleton assembly, and gene expression [1,2]. The RhoGAP activity resides in a conserved sequence domain of ~150 amino acids that enhances the hydrolysis of bound GTP to convert Rho proteins to their inactive state [3,4].

The rat p122 RhoGAP molecule and its human orthologue, DLC-1 (deleted in liver cancer 1), are ~120 kDa polypeptides that contain a RhoGAP domain [5,6] and two other potential functional domains, a sterile alpha motif (SAM) protein interaction domain and a lipid-binding StAR-related lipid-transfer (START) domain [7,8]. In vitro studies indicated that p122/DLC-1 can act as a GAP for RhoA and Cdc42 [5,9], and p122 also stimulated the hydrolysis of phosphatidylinositol 4,5-bisphosphate by phospholipase C-δ1 [5]. DLC-1 has tumor suppressor activity and has been shown to influence the morphology, adhesion, proliferation, and tumorigenicity of cultured cells [9–12]. To provide an animal model for investigating the biological functions of DLC-1, we have generated mice with a targeted disruption of the DLC-1 gene and found that loss of DLC-1 activity leads to embryonic lethality by midgestation.

2. Materials and methods

2.1. Localization of the DLC-1 transcript in mouse embryos

In situ hybridization of ^{35}S-labeled sense or antisense riboprobes to sections of wild type 10 days post coitum (dpc) mouse embryos was performed by Molecular Histology, Inc. (Gaithersburg, MD), using previously described methods [13]. The riboprobes were transcribed from mouse DLC-1 cDNA inserts in pBluescript (Stratagene).

2.2. Construction of a mouse DLC-1 gene targeting vector

The mouse DLC-1 genomic clone λG2 [14,15] was used as template to generate two DNA segments by PCR for insertion into the pPNT vector [16]. A 1.3-kb 5′ arm containing exon 4 was amplified using the primers 5′-ggaattccgagaagctcatattgtatg and 5′-cggatccgactgtcatttaaccagccc and ligated into the *Eco*RI/*Bam*HI sites of the vector. A 5.8-kb 3′ arm extending from intron 5 to part of exon 9 was amplified with the primers 5′-taatgtcgacctcccgatgtgcgtagacactatcc and 5′-taatgcggccgcggagtcatctggttttctttcacagc and cloned into the *Not*I/*Xho*I sites of the plasmid. The *Not*I-cut targeting vector was electroporated into the HM-1 embryonic stem (ES) cell line [17], and the cells were cultured in G418 and ganciclovir as described [18]. Southern blots of *Xba*I-cut genomic DNA from drug-resistant ES cell colonies were hybridized to a ^{32}P-labeled external probe in intron 3, which will detect *Xba*I bands of 3.5 kb in the wild type gene and 2.2 kb in the correctly targeted allele, due to the introduction of an *Xba*I site in pPNT. Four ES clones harboring the disrupted gene were identified and all yielded chimeric mice when injected into C57BL/6 blastocysts. The agouti progeny of chimeras mated with C57BL/6 mice were genotyped by Southern blot hybridization of tail biopsy DNA and also by PCR using two primer pairs: (1) a primer in the neomycin-resistance cassette of pPNT (5′-gcagcctctgttccacatacactt) and a primer from intron 4 (5′-gcaacacttggtcagacttctg), which amplify an ~130 bp product specific for the targeted allele; (2) primers from exon 5 (5′-acccattcagtcagtccacc and 5′-attgcgtctcttcagctcc), which amplify a 260-bp band from the wild type gene. The disrupted allele was maintained in the heterozygous state on a mixed C57BL/6 × 129/Ola background.

2.3. Northern blot analysis of DLC-1 mRNA

Total RNA was prepared from mouse tissues using the TRIzol reagent (Invitrogen) and analyzed by Northern blot hybridization as previously described [15]. The blot was probed with a ^{32}P-labeled 1.3-kb

*Corresponding authors. Fax: +1 301 496 0734.
E-mail addresses: marian_durkin@nih.gov (M.E. Durkin), popescun@mail.nih.gov (N.C. Popescu).

[1] Present address: Laboratory of Molecular Genetics, Toxicology and Molecular Biology Branch, Health Effects Laboratory Division, National Institute for Occupational Safety and Health, Morgantown, WV 26505, USA.

Abbreviations: DLC-1, deleted in liver cancer 1; dpc, days post coitum; ES, embryonic stem cell; GAP, GTPase-activating protein; SAM, sterile alpha motif; START, StAR-related lipid-transfer

0014-5793/$30.00
doi:10.1016/j.febslet.2004.12.090

*Hin*dIII fragment from exon 14 of the mouse DLC-1 gene [15] and then re-hybridized to a 376-bp mouse L19 ribosomal protein cDNA fragment as a control for loading.

2.4. Histological analysis of mutant embryos

Embryos from matings of DLC-1$^{+/-}$ mice were dissected from the uterine horns on 12.5, 10.5, and 9.5 dpc, and the yolk sacs were reserved for DNA preparation and genotyping. Placentae and 9.5 dpc embryos were fixed in 10% neutral buffered formalin, and 12.5 and 10.5 dpc embryos were placed in Bouin's fixative. Sections were stained with hematoxylin/eosin (H&E) for microscopic examination.

2.5. Mouse embryo fibroblast cultures

Embryos from intercross matings were removed on 9.5 dpc, and the cells were dissociated by trypsinization and cultured in Dulbecco's modified Eagles medium supplemented with 10% FBS and antibiotics. Cells were genotyped by PCR, and studies were performed on wild type and DLC-1$^{-/-}$ cells prior to passage 10. Subconfluent cultures plated on glass coverslips were incubated for 12 h in medium containing 0.5% fetal bovine serum prior to fixation with 10% neutral buffered formalin. Staining of actin fibers with Texas Red®-X phalloidin was performed according the manufacturer's protocol (Molecular Probes, Eugene, OR). Focal adhesions were visualized by indirect immunofluorescence using anti-vinculin monoclonal antibody (V9131, Sigma) and FITC-conjugated anti-mouse IgG (Sigma F9887), both diluted 1/100. Vinculin-stained cells were grown on coverslips coated with 10 μg/ml fibronectin. The preparations were examined on a Zeiss Axiophot epifluorescent microscope equipped with the appropriate filters, and selected areas were recorded as 16-bit grayscale images on a Photometrics CoolSNAP monochrome camera controlled by an Apple Macintosh computer. Digital images were analyzed and pseudocolored by IPLab 3.6.2 software (Scanalytics, Inc., Fairfax, VA).

3. Results

3.1. Localization of the DLC-1 transcript in mouse embryos

DLC-1 mRNA is widely expressed in adult mouse tissues [15] and was detected in 9.5 dpc embryos by RT-PCR (not shown). In situ hybridization showed that the DLC-1 transcript was present in a number of tissues in 10 dpc embryos, although the levels were relatively low in the neuroepithelium of the brain and neural tube (Fig. 1A and B). In the placenta, DLC-1 mRNA was enriched in the trophoblast cells of the spongiotrophoblast and labyrinth compared to the maternal decidua (Fig. 1C and D).

3.2. Targeted disruption of the mouse DLC-1 gene

The mouse DLC-1 gene (*Arhgap7*) consists of 14 exons spanning 50 kb on mouse chromosome 8 [14,15]. To inactivate the gene by homologous recombination, a targeting vector was designed to delete exon 5 (Fig. 2), which encodes a serine-rich domain of the protein. Loss of the 1427-bp exon 5 will cause a reading frame shift that will result in premature translation termination and synthesis of a truncated polypeptide containing the first 77 amino acids of the DLC-1 protein, which comprises the SAM domain, plus 23 novel residues due to the altered reading frame. Two independent ES cell lines generated mice capable of germline transmission of the targeted DLC-1 allele. When DLC-1$^{+/-}$ mice were crossed, no homozygous mutant offspring were obtained, indicating that DLC-1$^{-/-}$ embryos died in utero. Embryos of all three genotypes were observed at 10.5 dpc (Fig. 2D).

3.3. Characterization of mice heterozygous for the targeted DLC-1 gene

Adult DLC-1$^{+/-}$ mice did not display any gross physical or behavioral abnormalities, and histopathological analysis of tissues from seven-month old mice (performed by the Pathology Phenotyping Service of the Veterinary Resources Program, Office of Research Services, National Institutes of Health, Bethesda, MD) did not reveal any lesions specific for the heterozygous animals. On Northern blots, there was a reduction in the level of the wild type 6.5-kb DLC-1 mRNA in tissues of DLC-1$^{+/-}$ animals but no sign of an ~5.1-kb transcript expected from the mutated allele (Fig. 3). The DLC-1 transcript lacking exon 5 may be targeted for degradation by the non-

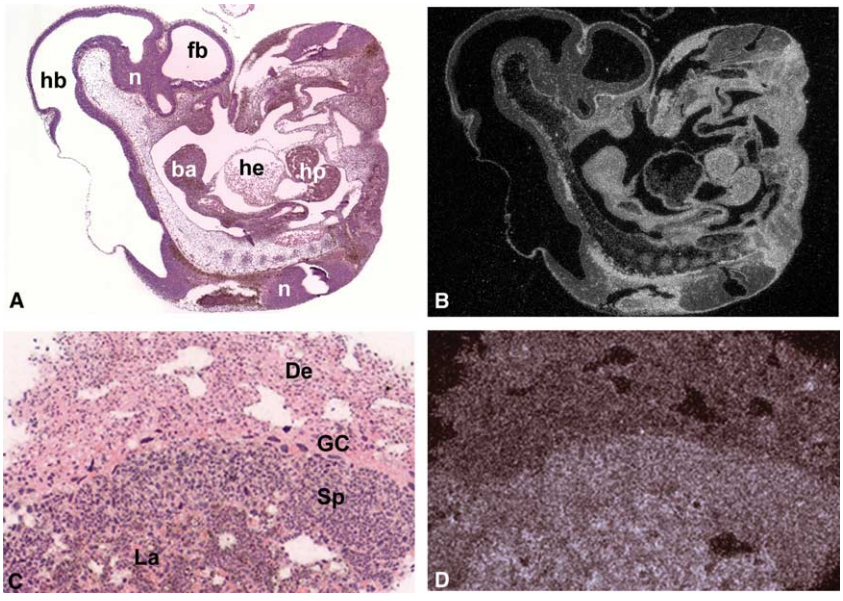

Fig. 1. Localization of the DLC-1 transcript in mouse embryos on 10 dpc by in situ hybridization. Bright-field (A) and dark-field (B) images of a sagittal section through embryo: ba, branchial arch; fb, forebrain; hb, hindbrain; he, heart; hp, hepatic primordia; n, neuroepithelium. Bright-field (C) and dark-field (D) images of placenta. De, decidua; GC, giant cells; Sp, spongiotrophoblast; La, labyrinth.

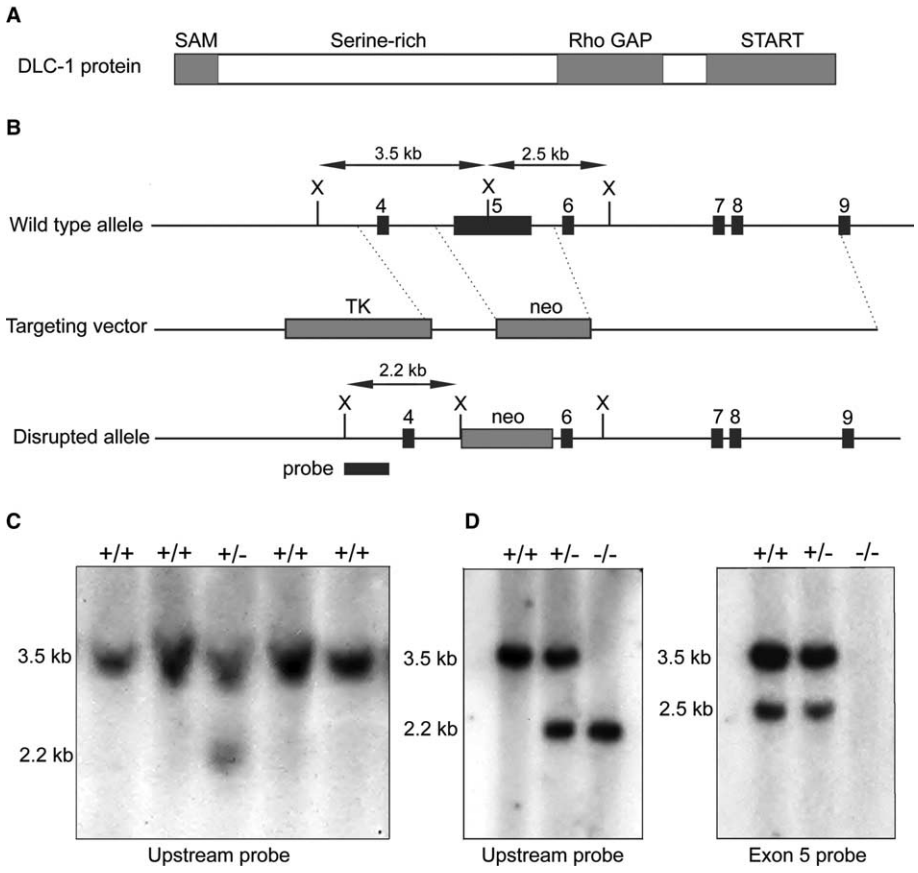

Fig. 2. Targeted mutation of the mouse DLC-1 gene. (A) Diagram of the structural organization of the 1084-amino acid mouse DLC-1 polypeptide [15], showing the SAM, serine-rich, RhoGAP, and START domains. (B) Schematic representation of the central region of the wild type *Arhgap7* locus, the targeting vector, and the targeted allele. Exons are indicated by numbered boxes, and *Xba*I sites (X) in the genomic DNA and the pPNT vector are shown. Gray boxes denote the herpes simplex virus thymidine kinase (TK) and the bacterial neomycin-resistance (neo) cassettes of pPNT. A solid box indicates the location of the probe used for Southern blot hybridization. (C) A Southern blot of *Xba*I-cut genomic DNA from drug-resistant ES cell colonies, showing hybridization of the probe to the 2.2 kb band characteristic of the disrupted gene in one clone. (D) Southern blot of *Xba*I-digested yolk sac DNA from 10.5 dpc embryos obtained from an intercross mating. Hybridization to the upstream probe indicated the presence of wild type (+/+), heterozygous (+/−), and homozygous (−/−) mutant littermates. On the right, the same blot was stripped and reprobed with a ^{32}P-labeled fragment from exon 5, to confirm the deletion of this exon in the DLC-1$^{-/-}$ embryo.

sense-mediated decay mechanism that eliminates mRNA species with premature translation termination codons [19] and may not yield significant amounts of a truncated protein.

3.4. Abnormalities in DLC-1$^{-/-}$ embryos

Histological analysis of embryos from intercross matings showed that DLC-1$^{-/-}$ embryos were absent or necrotic on 12.5 dpc (not shown). At 10.5 and 9.5 dpc homozygotes displayed defects in several organ systems, which varied in severity. One embryo at 9.5 dpc lacked the forebrain and had incomplete morphogenesis of the hindbrain, branchial arches, and heart (Fig. 4B and E). In a second DLC-1$^{-/-}$ embryo from the same litter, organogenesis had progressed further but was aberrant; the anterior neural tube was open and contorted, the hindbrain had a narrow lumen with a hyperplastic neuroepithelium, and the branchial arches and the chambers of the heart were distorted (Fig. 4C and F). Placental development was also affected by DLC-1 deficiency (Fig. 5). The wild type placental labyrinth at 10.5 dpc contains sinusoids with maternal enucleated red blood cells and embryonic blood vessels with nucleated fetal erythrocytes. In DLC-1$^{-/-}$ placentae, formation of the embryonic vasculature was reduced, and clusters

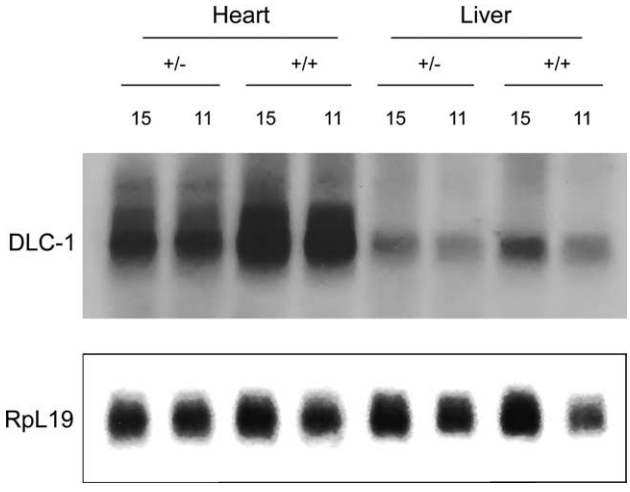

Fig. 3. Comparison of DLC-1 mRNA in wild type and heterozygous mutant mice. Northern blot of liver and heart total RNA (20 μg per lane), isolated from matched wild type (+/+) and heterozygous (+/−) siblings from two litters, 15 and 11. The same blot was hybridized sequentially to a DLC-1 cDNA probe and a mouse ribosomal protein L19 cDNA probe (RpL19).

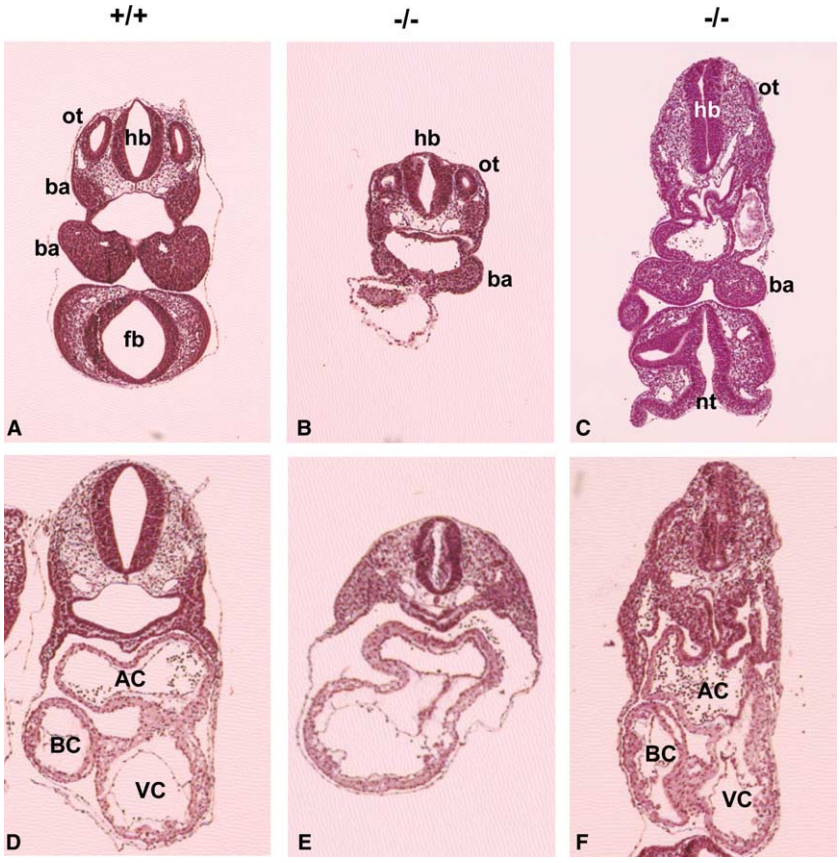

Fig. 4. Abnormal development of DLC-1$^{-/-}$ embryos. Serial transverse H&E stained sections of three 9.5 dpc embryos from the same litter; embryo 1 is wild type (+/+), and embryos 5 and 6 were homozygous for the targeted DLC-1 allele (−/−). (A) Section of embryo 1 at level of branchial arches (ba). The forebrain (fb), hindbrain (hb), and otic pits (ot) are indicated. (B) Section of embryo 6 at a similar level, showing lack of forebrain and incomplete development of branchial arches. (C) Section of embryo 5 at level of branchial arches; note open neural tube (nt) in the forebrain and disorganization of the branchial arches, the hind brain neuroepithelium, and the otic pit. (D) Section through heart of embryo 1. AC, common atrial chamber; BC, bulbus cordis; VC, ventricular chamber. (E) Section through heart of embryo 6, showing incomplete formation of the chambers. (F) Section through heart of embryo 5, in which the architecture of the chambers is distorted.

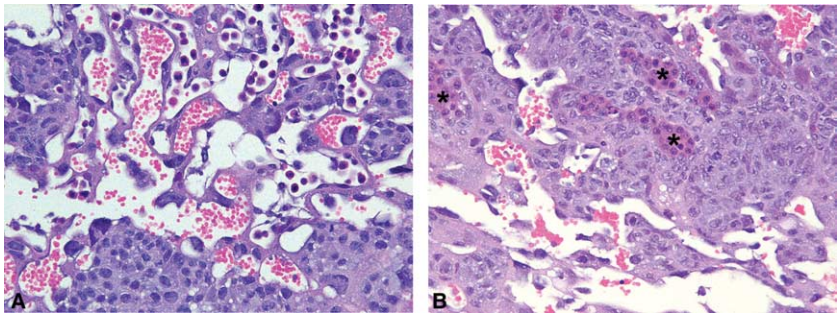

Fig. 5. Placental defects in DLC-1$^{-/-}$ embryos. (A) H&E stained section of placental labyrinth of wild type 10.5 dpc embryo sinuses with maternal red blood cells are adjacent to embryonic blood vessels containing nucleated fetal erythrocytes. (B) Placenta of DLC-1$^{-/-}$ littermate embryo has reduced vascularization of the labyrinth. Defective embryonic blood vessels contain immature fetal erythrocytes (asterisks).

of immature erythrocytes in collapsed blood vessels were observed in the trophoblast layer.

3.5. Cytoskeleton alterations in DLC-1$^{-/-}$ mouse embryo fibroblasts

Fibroblasts isolated from 9.5 dpc DLC-1$^{-/-}$ embryos were viable and able to proliferate in culture, but the organization of cytoskeletal proteins differed from that of cells from wild type embryos (Fig. 6). The DLC-1-deficient cells had fewer long actin stress fibers and a reduced number of focal adhesion-like structures when stained with antibodies against vinculin, an actin-binding protein present in focal adhesions [20].

4. Discussion

Spontaneous and targeted mutations of genes encoding proteins involved in Rho GTPase signaling pathways produce a range of phenotypes, including neurological disorders in humans [2,3]. In this communication, we report that DLC-1, a

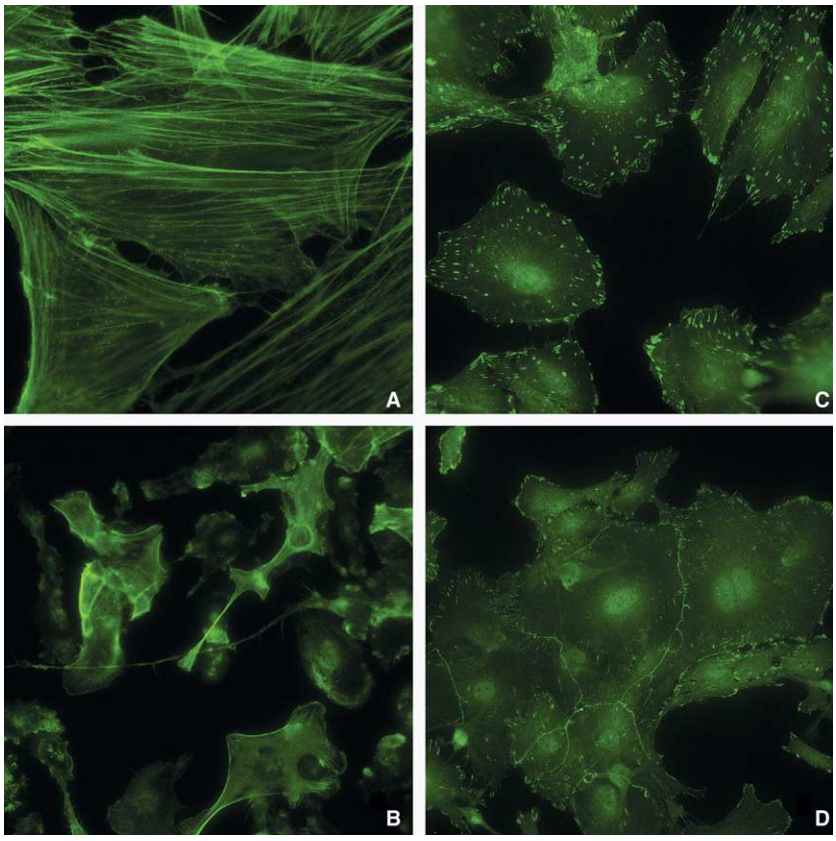

Fig. 6. Altered cytoskeletal organization in DLC-1-deficient mouse embryo fibroblasts. Cells from wild type (A, C) and DLC-$1^{-/-}$ (B, D) littermate embryos were stained with fluorescent phalloidin (A, B) and anti-vinculin antibodies (C, D).

candidate tumor suppressor gene, has a critical role in regulating cellular functions during early murine development. The DLC-1-deficient embryos were found to have neural tube defects, but these are a common occurrence in mouse gene knockouts that result in death at early to midgestation and may be secondary to failure of other organ systems [21]. Lethality at this stage is often due to placental or cardiac defects [22,23]. Abnormalities in both tissues were found in homozygous DLC-1 mutant embryos, at a developmental stage when the DLC-1 transcript is normally expressed, and the primary cause of embryonic death is not known.

Recently, p122/DLC-1 has been localized to focal adhesions [24], sites at which extracellular matrix receptors are linked to the actin cytoskeleton and which contain numerous regulatory and structural proteins [20,25]. We have shown that the formation of actin stress fibers and vinculin-rich focal adhesions was reduced in DLC-$1^{-/-}$ mouse embryo fibroblasts. DLC-1 has been implicated in the phosphoinositide and Rho GTPase signaling pathways, both of which regulate stress fiber and focal adhesion assembly [2,10,26], and loss of DLC-1 may interfere with development by adversely affecting cell adhesion and migration.

Two human genes have been identified that encode proteins closely related to DLC-1, KIAA0189/STARD8 [27] and DLC2/STARD13 [28]. The mouse orthologues of the DLC-1-like proteins are apparently unable to compensate during embryogenesis for the lack of DLC-1, due to divergent functions or different expression patterns. The reduced DLC-1 mRNA levels in heterozygotes appear to be compatible with normal development; however, DLC-1 haploinsufficiency might produce phenotypic changes on a different genetic background or after challenge with carcinogens or other agents.

Acknowledgments: We thank Anita Ton for culturing of ES cells; Dr. Jerrold M. Ward for analysis of the placental phenotype; Dr. Mark A. Bryant for histopathological evaluation of adult mice; Dr. Glenn Merlino for helpful advice and Shauna Everett for photographic assistance.

References

[1] Zohn, I.M., Campbell, S.L., Khosravi-Far, R., Rossman, K.L. and Der, C.J. (1998) Rho family proteins and Ras transformation: the RHOad less traveled gets congested. Oncogene 17, 1415–1438.
[2] Boettner, B. and Van Aelst, L. (2002) The role of Rho GTPases in disease development. Gene 286, 155–174.
[3] Moon, S.Y. and Zheng, Y. (2003) Rho GTPase activating proteins in cell regulation. Trends Cell Biol. 13, 13–22.
[4] Peck, J., Douglas 4th, G., Wu, C.H. and Burbelo, P.D. (2002) Human RhoGAP domain-containing proteins: structure, function, and evolutionary relationships. FEBS Lett. 528, 27–34.
[5] Homma, Y. and Emori, Y. (1995) A dual functional signal mediator showing RhoGAP and phospholipase C-δ1 stimulating activities. EMBO J. 14, 286–291.
[6] Yuan, B.-Z., Miller, M.J., Keck, C.L., Zimonjic, D.B., Thorgeirsson, S.S. and Popescu, N.C. (1998) Cloning, characterization, and chromosomal localization of a gene frequently deleted in human liver cancer (*DLC-1*) homologous to rat *RhoGAP*. Cancer Res. 58, 2196–2199.
[7] Schultz, J., Ponting, C.P., Hofmann, K. and Bork, P. (1997) SAM as a protein interaction domain involved in developmental regulation. Prot. Sci. 6, 249–253.
[8] Ponting, C.P. and Aravind, L. (1999) START: a lipid-binding domain in StAR, HD-ZIP and signalling proteins. Trends Biochem. Sci. 24, 130–132.

[9] Wong, C.-M., Lee, J.M., Ching, Y.-P., Jin, D.-Y. and Ng, I.O. (2003) Genetic and epigenetic alterations of DLC-1 gene in hepatocellular carcinoma. Cancer Res. 63, 7646–7651.
[10] Sekimata, M., Kabuyama, Y., Emori, Y. and Homma, Y. (1999) Morphological changes and detachment of adherent cells induced by p122, a GTPase activating protein for Rho. J. Biol. Chem. 274, 17757–17762.
[11] Ng, I.O., Liang, Z.-D., Cao, L. and Lee, T.K. (2000) *DLC-1* is deleted in primary hepatocellular carcinoma and exerts inhibitory effects on the proliferation of hepatoma cell lines with deleted *DLC-1*. Cancer Res. 60, 6581–6584.
[12] Yuan, B.-Z., Zhou, X., Durkin, M.E., Zimonjic, D.B., Gumundsdottir, K., Eyfjord, J.E., Thorgeirsson, S.S. and Popescu, N.C. (2003) DLC-1 gene inhibits human breast cancer cell growth and in vivo tumorigenicity. Oncogene 22, 445–450.
[13] Hoover, S.B., Sung, C., Cottler-Fox, M. and Fox, C.H. (2000) In situ hybridization techniques for studying gene expression in the genetically altered mouse in: Pathology of Genetically Engineered Mice (Ward, J.M., Mahler, J.F., Maronpot, R.R., Sundberg, J.P. and Frederickson, R.M., Eds.), pp. 13–22, Iowa State University Press, Ames, IA.
[14] Yuan, B.-Z., Yang, Y., Keck-Waggoner, C.L., Zimonjic, D.B., Thorgeirsson, S.S. and Popescu, N.C. (1999) Assignment and cloning of mouse *Arhgap7* to chromosome 8A4-B2, a conserved syntenic region of human chromosome 8p22-p21. Cytogenet. Cell Genet. 87, 189–190.
[15] Durkin, M.E., Yuan, B.-Z., Thorgeirsson, S.S. and Popescu, N.C. (2002) Gene structure, tissue expression, and linkage mapping of the mouse DLC-1 gene (*Arhgap7*). Gene 288, 119–127.
[16] Tybulewicz, V.L., Crawford, C.E., Jackson, P.K., Bronson, R.T. and Mulligan, R.C. (1991) Neonatal lethality and lymphopenia in mice with a homozygous disruption of the c-abl proto-oncogene. Cell 65, 1153–1163.
[17] Selfridge, J., Pow, A.M., McWhir, J., Magin, T.M. and Melton, D.W. (1992) Gene targeting using a mouse HPRT minigene/HPRT-deficient embryonic stem cell system: inactivation of the mouse *ERCC-1* gene. Somat. Cell Mol. Genet. 18, 325–336.
[18] Jensen, M.R., Factor, V.M., Fantozzi, A., Helin, K., Huh, C.-G. and Thorgeirsson, S.S. (2003) Reduced hepatic tumor incidence in cyclin G1-deficient mice. Hepatology 37, 862–870.
[19] Byers, P.H. (2002) Killing the messenger: new insights into nonsense-mediated mRNA decay. J. Clin. Invest. 109, 3–6.
[20] Petit, V. and Thiery, J.-P. (2000) Focal adhesions: structure and dynamics. Biol. Cell 92, 477–494.
[21] Harris, M.J. and Juriloff, D.M. (1999) Mini-review: Toward understanding mechanisms of genetic neural tube defects in mice. Teratology 60, 292–305.
[22] Copp, A.J. (1995) Death before birth: clues from gene knockouts and mutations. Trends Genet. 11, 87–93.
[23] Ward, J.M. and Devor-Henneman, D.E. (2000) Gestational mortality in genetically engineered mice: evaluating the extraembryonal embryonic placenta and membranes in: Pathology of Genetically Engineered Mice (Ward, J.M., Mahler, J.F., Maronpot, R.R., Sundberg, J.P. and Frederickson, R.M., Eds.), pp. 103–122, Iowa State University Press, Ames, IA.
[24] Kawai, K., Yamaga, M., Iwamae, Y., Kiyota, M., Kamata, H., Hirata, H., Homma, Y. and Yagisawa, H. (2004) A PLCδ1-binding protein, p122RhoGAP, is localized in focal adhesions. Biochem. Soc. Trans. 32, 1107–1109.
[25] DeMali, K.A., Wennerberg, K. and Burridge, K. (2003) Integrin signaling to the actin cytoskeleton. Curr. Opin. Cell Biol. 15, 572–582.
[26] Toker, A. (1998) The synthesis and cellular roles of phosphatidylinositol 4,5-bisphosphate. Curr. Opin. Cell Biol. 10, 254–261.
[27] Nagase, T., Seki, N., Ishikawa, K., Tanaka, A. and Nomura, N. (1996) Prediction of the coding sequences of unidentified human genes. V. The coding sequences of 40 new genes (KIAA0161–KIAA0200) deduced by analysis of cDNA clones from human cell line KG-1. DNA Res. 3, 17–24.
[28] Ching, Y.-P., Wong, C.-M., Chan, S.-F., Leung, T.H., Ng, D.C., Jin, D.-Y. and Ng, I.O. (2003) Deleted in liver cancer (DLC) 2 encodes a RhoGAP protein with growth suppressor function and is underexpressed in hepatocelluar carcinoma. J. Biol. Chem. 278, 10824–10830.